

How to constrain warm dark matter with the Lyman α forest

Antonella Garzilli,^{1,2*} Andrii Magalich,³ Oleg Ruchayskiy² and Alexey Boyarsky³

¹EPFL Laboratoire d'astrophysique, Observatoire de Sauvigny, CH-1290 Versoix, Switzerland

²Niels Bohr Institute, Copenhagen University, Blegdamsvej 17, DK-2100 Copenhagen, Denmark

³Lorentz Institute, Leiden University, Niels Bohrweg 2, Leiden, NL-2333 CA, The Netherlands

Accepted 2021 January 20. Received 2021 January 20; in original form 2019 December 19

ABSTRACT

The flux power spectrum of the high resolution Lyman- α forest data exhibits suppression at small scales. The origin of this suppression can be due to long-sought warm dark matter (WDM) or to thermal effects, related to the largely unknown reionization history of the Universe. Previous works explored a specific class of reionization histories that exhibit sufficiently strong thermal suppression and leave little room for warm dark matter interpretation. In this work we choose a different class of reionization histories, fully compatible with available data on evolution of reionization, but much colder than the reionization histories used by previous authors in determining the nature of dark matter, thus leaving the broadest room for the WDM interpretation of the suppression in the flux power spectrum. We find that WDM thermal relics with masses below 1.9 keV (95% CL) would produce a suppression at scales that are larger than observed maximum of the flux power spectrum, independently of assumptions about thermal effects. This WDM mass is significantly lower than previously claimed bounds, demonstrating the level of systematic uncertainty of the Lyman- α forest method, due to the previous modelling. We also discuss how this uncertainty may affect also data at large scales measured by eBOSS.

1 WARM DARK MATTER AND LYMAN- α FOREST

Dark matter in the Universe manifests itself through many distinct observations – from rotational curves of stars in galaxies to the statistics of anisotropies of cosmic microwave background Peebles (2017). If dark matter is made of particles – little is known about their properties. In particular, it is not known whether dark matter is *warm* – *i.e.* was born relativistic – as opposed to *cold dark matter* (CDM). While warm dark matter (WDM) was cooling with expansion, it erased primordial inhomogeneities at scales below its *free streaming* horizon, λ_{DM} . This means that the growth of structures in warm dark matter is suppressed. The main distinction between CDM and WDM lies thus in the suppression of the matter power spectrum below a certain scale.

One of the promising tools to measure dark matter distribution at small scales is the *Lyman- α forest method* – a set of absorption features in the spectra of background quasars due to the Lyman- α ($n = 1 \rightarrow 2$) transition in the rest frame of neutral hydrogen clouds at redshifts $2 \leq z \leq 5$ (Meiksin 2009). Under the assumption that neutral hydrogen traces matter distribution, it allows to measure a proxy of the matter power spectrum (known as *flux power spectrum*, FPS). The method has been actively used to explore the properties of dark matter particles (Hansen et al. 2002; Viel et al. 2005, 2006; Seljak et al. 2006; Viel et al. 2008; Boyarsky et al. 2009a; Boyarsky et al. 2009b; Viel et al. 2013; Garzilli et al. 2017; Iršič et al. 2017; Murgia et al. 2018; Baur et al. 2016, 2017; Garzilli et al. 2019; Palanque-DeLabrouille et al. 2020).

The effect of warm dark matter gets more pronounced at smaller scales. Therefore, Lyman- α forest data based on spectra of high spectral resolution ($\mathcal{R} \equiv \lambda/\Delta\lambda \sim 60'000$) are of special interest as they allow to probe FPS down to scales $k \sim 0.1 - 0.2$ s/km, see Garzilli et al. (2019). The observed flux power spectrum Δ_F^2 exhibits a sharp suppression at comoving wave-number above $k_F \sim 0.03$ s/km (Boera et al. 2019). The same cutoff is visible in the older

dataset based on HIRES (Vogt et al. 1994) and MIKE (Bernstein et al. 2002) quasar spectra (Viel et al. 2013).

1.1 Degeneracy between WDM and thermal effects

The presence of the cut-off in the high resolution data does not mean, however, that warm dark matter with $\lambda_{\text{DM}} \sim \lambda_F$ has been discovered! Indeed, several thermal effects may prevent H I from following dark matter distribution at small scales. These effects are *degenerate* with that of warm dark matter. This makes the derivation of robust WDM bounds from the high resolution Lyman- α data problematic, as we will discuss in details below.

Doppler broadening. Intergalactic medium (IGM) is heated during reionization. The temperature of the intergalactic medium depends on the density and follows the *temperature-density relation* (Hui & Rutledge 1999):

$$T = T_0(z) \left(\frac{\rho}{\bar{\rho}} \right)^{\gamma(z)-1} \quad (1)$$

where ρ is the matter density of a small patch of the Universe and $\bar{\rho}$ is the background matter density. Both parameters T_0 and γ are functions of redshift. The non-zero temperature and thus the Maxwellian velocities of the gas particles cause the Doppler broadening of the absorption lines. This introduces its own cutoff in the flux power spectrum. The temperature of the gas, and hence the scale of the Doppler (temperature) broadening, λ_b is not accurately known (see e.g. Garzilli et al. 2017; Rorai et al. 2018), especially at redshifts $z \gtrsim 5$ (Hui & Haiman 2003; Bolton et al. 2010; Becker et al. 2011; Bolton et al. 2012; Lidz & Malloy 2014; Walther et al. 2018, 2019). Therefore, in deriving WDM bounds one marginalizes over $T_0(z)$ and $\gamma(z)$.

The high resolution HIRES/MIKE data were used to derive Lyman- α constraints by Viel et al. (2013). Assuming a particular

family of reionization histories (Haardt & Madau 2001, 2012) combined with a powerlaw ansatz for the $T_0(z)$ for $3 \leq z \leq 6$, the constrain $m_{\text{WDM}} \geq 3.3$ keV was found.¹ This would correspond to the cutoff scale $\lambda_{\text{dm}} \lesssim 30$ ckpc.

These bounds were revisited in (Garzilli et al. 2017). It was argued that the IGM temperature is poorly constrained at redshifts $z \sim 5$ and may not be monotonous (due to combination of adiabatic cooling and HeII reionization starting at later times). By allowing $T_0(z)$ to be non-monotonous at $z = 4 - 6$, Garzilli et al. (2017) demonstrated that the data can be fit by the WDM model with $m_{\text{WDM}} \approx 2.1$ keV or by the CDM (*i.e.* the two models could not be distinguished by the data). The fact that their bounds weaken if $T_0(z)$ is allowed to vary independently in each redshift bin has been acknowledged by Viel et al. (2013) who did not find, however, statistical evidence in favour of it and chose to quote a less conservative WDM bound, see Garzilli et al. (2017) for discussion.

Re-analysis of the same data with higher resolution of simulations, different modeling of ultra-violet background (Iršič et al. 2017) changed the bound to around $m_{\text{WDM}} \geq 3.9 - 4.1$ keV or confirmed our findings, depending on the choice of priors on thermal history.

Later works (Walther et al. 2018, 2019; Boera et al. 2019) indeed confirmed that IGM temperature reaches a local minimum around $z \sim 5$.

Pressure effects. The proper inclusion of the temperature effects did not however, exhausts all possible uncertainties of the WDM bounds. Inceed, as the absorbing filaments in the IGM are not virialize structures, their typical size depends on the past thermal history, relatively to the time of observation. The gas distribution is smoothed compared to the dark matter due to pressure (Gnedin & Hui 1998; Theuns et al. 2000; Kulkarni et al. 2015; Upton Sanderbeck et al. 2016)

In the absence of realistic first-principle modeling of reionization, one has to run hydrodynamical simulations with pre-defined photo-heating and photo-ionization rates in order to assess the influence of each specific thermal history onto the Lyman- α observables. Properly quantifying systematic effects of all admissible reionization histories would require running a prohibitively large grid of hydrodynamical simulations.

The work Garzilli et al. (2019) demonstrated that the observed shape of the high-resolution FPS and its redshift evolution can be explained equally well by either CDM plus Haardt & Madau (2012) reionization history, or by warm dark matter plus a reionization history of Oñorbe et al. (2017a) that has a lower scale λ_p still perfectly consistent with the data. The work did not put specific bounds, but rather illustrated that the degeneracy between astrophysical and warm dark matter is much stronger than assumed in the previous works. This degeneracy cannot be resolved by the current data (although many interesting ideas exist on how this can be done (see e.g. Garzilli et al. 2015, 2020; Gaikwad et al. 2020)

Until this is done – *unknown reionization history represents the major systematic uncertainty in deriving bounds on WDM mass.*

Current work makes a new step in evaluating these uncertainties.

¹ In this work by “WDM” we refer to a specific class where DM is produced in thermal equilibrium, and then freezes out – (*warm*) *thermal relics* or “thermal WDM” (Bode et al. 2001). In this case there is a one-to-one relation between λ_{DM} and the DM particle mass, m_{WDM} ($\lambda_{\text{DM}} \propto m_{\text{WDM}}^{-4/3}$), (see e.g. Boyarsky et al. 2009b). Although “thermal WDM” does not correspond to any specific particle physics model, such a parametrization of WDM is often chosen when deriving constraints. We use it in our paper to facilitate comparison with other works.

In order to quantify the uncertainty, we find a reionization history with the smallest pressure support scale, λ_p (Oñorbe et al. 2017a). By pushing all astrophysical effects to their minimum, we try to describe the cut-off in the data by the warmest possible DM model. In this way, we identify the WDM model whose cut-off scale is larger than $\lambda_F \sim 30$ (s/km)⁻¹ and is, therefore, ruled out independently of astrophysical assumptions. Therefore, when allowing for the wider class of reionization histories, the WDM bound relaxes down to 1.9 keV (which represents a factor of ≈ 3 increase of the characteristic cut-off scale, $\lambda_{\text{DM}} \lesssim 100$ ckpc). This results is defined by the scale of the cut-off observed in the data, the bound can not be improved unless the origin of the cut-off is proven to be astrophysical.

Other WDM bounds. If the bounds from high-redshift data indeed have large uncertainty – can other data provides more robust bounds? The Lyman- α data with medium spectral resolution ($\mathcal{R} \sim 2'200$), coming *e.g.* from the SDSS (BOSS, eBOSS) surveys has been used to constrain WDM (Viel et al. 2006; Seljak et al. 2006; Viel et al. 2008; Boyarsky et al. 2009a; Boyarsky et al. 2009b; Baur et al. 2016, 2017; Palanque-Delabrouille et al. 2020). These data allow to probe comoving wave-numbers up to $k_{\text{sdss}} \approx 0.02$ sec/km. The most recent bound using the SDSS DR14 (eBOSS) data was claimed to be $m_{\text{WDM}} \gtrsim 5.3$ keV at 95%CL (Palanque-Delabrouille et al. 2020). Both temperature and pressure effects operate at scales smaller than k_{sdss}^{-1} . Palanque-Delabrouille et al. (2020) limits WDM by requiring that its deviation from CDM (inferred from large-scale cosmological observations) at scales above the cut-off ($k < k_{\text{sdss}}$) would be “within errorbars”. Statistical errorbars of the eBOSS data are small, owing to large number of observed quasars and the bound based on these statistical errors appear to be quite tight. We arrive to a paradoxical conclusion that the scales where WDM effects are small (at $k < k_{\text{sdss}} < k_F$) are more sensitive than the scales where they are large ($k > k_F$, high-resolution data). This conclusion relies however on the fact that the sensitivity of the eBOSS data is defined by statistical rather than systematic uncertainties. To make this conclusion one needs to model astrophysical effects in great detail. In particular, if pressure effects and effects of warm dark matter are of the same order at scales $k > k_F$ (Garzilli et al. 2019), one should demonstrate that their k dependence is different. Otherwise, two models: “CDM plus larger λ_p ” and “WDM plus smaller λ_p ” that were indistinguishable at $k > k_F$ will be indistinguishable also at $k < k_{\text{sdss}}$. Palanque-Delabrouille et al. (2020) and previous works (Viel et al. 2006; Seljak et al. 2006; Viel et al. 2008; Boyarsky et al. 2009a; Boyarsky et al. 2009b; Baur et al. 2016, 2017) did not perform such an analysis. In particular, they did not explore in their work the full range of possible reionization histories, including “Late” versions of (Oñorbe et al. 2017a,b). They limited their redshift of reionization to $z_{\text{reio}} > 7$, while the recent data suggests that hydrogen reionization might have started at $z_{\text{reio}} < 7$ (Oñorbe et al. 2017a,b; Walther et al. 2019; Boera et al. 2019)) and was completed by $z = 5.7$ (Becker et al. 2015; Schroeder et al. 2013; Becker et al. 2001). We see therefore, that although formally stronger, *bounds based on eBOSS data are not free from systematic uncertainties due to unknown reionization history.*

Below we derive the bounds on the WDM particle mass using the high resolution Lyman- α data and the reionization history from (Oñorbe et al. 2017a) with the smallest pressure effects. We use the high-resolution data from Boera et al. (2019). This dataset is a re-observation with longer exposure of the quasar spectra already covered by the dataset of (Viel et al. 2013) (for their comparison see Appendix C of Boera et al. (2019)). We find that WDM models with

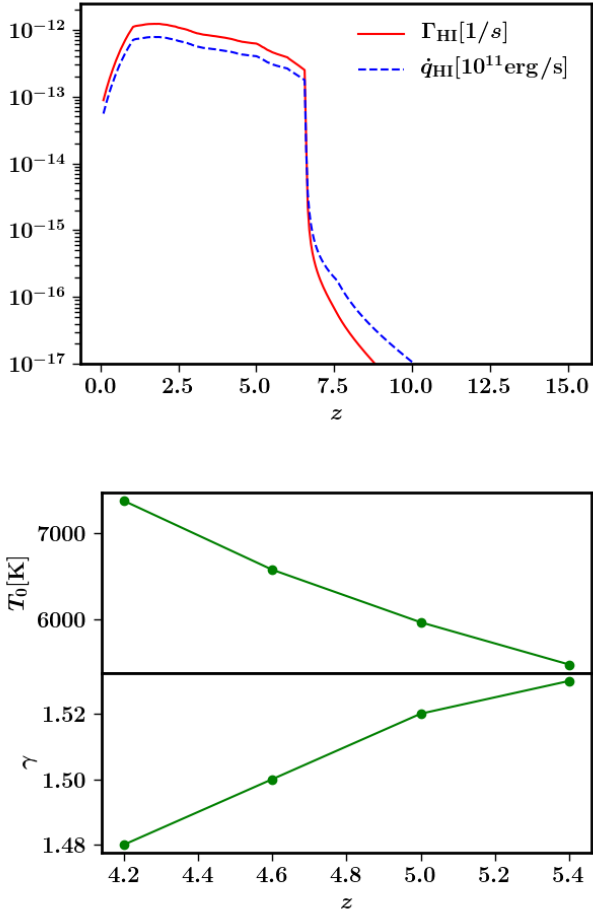


Figure 1. The adopted thermal history. In the upper panel we show the photoionization (Γ_{HI}) and photoheating (\dot{q}_{HI}) rates for the neutral hydrogen (HI) from the LATECOLD model of Oñorbe et al. (2017a). The photoheating rate is rescaled by 10^{11} in order to fit onto the same plot. The reionization in this model starts at $z_{\text{reio}} = 6.7$. In the lower panel we show the resulting temperature at the cosmic mean density of the IGM, T_0 , as well as the slope of the temperature-density relation, $\gamma(z)$ (obtained by fitting the Eq. (1) to the simulation snapshots).

1.9 keV have cut-off at scales around maximum of FPS ($k \sim k_F \approx 0.03$ s/km) and are therefore ruled out independently of astrophysical assumptions.

2 OUR METHOD

We start with a reionization history that provides smallest pressure support ($\lambda_p \ll \lambda_F$) and marginalize over the Doppler broadening and over the τ_{eff} . In this way we arrive to a model where *all astrophysical effects are pushed to the minimal level* and thus there is the broadest room for WDM effect. In more details our procedure is the following:

(1) In order to minimise the pressure effects, we run hydrodynamical simulations using the model of ultraviolet background (UVB)

LATECOLD (Oñorbe et al. 2017a).² We have summarized the simulations in Table 1, with cosmological parameters listed in Table 2. In this model the reionization starts at redshift $z = 6.7$, later than other thermal histories, considered in Oñorbe et al. (2017a) or by other groups. Nevertheless, LATECOLD scenario reproduces the measured temperature at post-reionization redshift $z \sim 5$ compatible with the constraint on reionization time Oñorbe et al. (2017a). By construction it gives the minimal filaments size.³ HI photo-heating and photo-ionization rates are shown in Fig. 1. We have assumed that the intergalactic medium is optically thin, and that reionization happens uniformly in all the space.

(2) We explicitly marginalise over the IGM temperature (*Doppler broadening*) adding their effects to the FPS in post-processing. Because the Lyman α forest at each redshift is sensitive only to a short range of densities, we model the IGM temperature with a single value, T_0 of the temperature-density relation (1). This is additionally justified by the fact that in the approximation of instantaneous reionization, that we are using, all the part of the IGM get to the same temperature at the same time, hence $\gamma = 1.0$, *i.e.*, there is no dependence of temperature on density.

(3) We also marginalise over the *effective optical depth* $\tau_{\text{eff}} = -\ln\langle F \rangle$, where F is the transmitted flux, and $\langle \dots \rangle$ is the average. τ_{eff} encompasses the information about the average absorption level (*i.e.* overall level of ionization of the IGM). The work Boera et al. (2019) provided measurements of τ_{eff} in each of the redshift bins together with the errorbars. We can vary τ_{eff} in the post-processing of the spectra, by rescaling the optical depth in the spectra by a suitable factor.

2.1 Data and Covariance matrix

The HIRES sample of high resolution quasar spectra at $z > 4$, released by Boera et al. (2019), consists of 15 Lyman α forest spectra over the redshift range $4.0 \leq z \leq 5.2$. These spectra are binned into three redshift intervals of width $\Delta z = 0.4$, centered on $z = 4.2, 4.6, 5.0$. Their total comoving length per redshift interval is $L = 1412, 2501, 1307$ Mpc/h. By construction the Lyman- α data points are strongly correlated Rollinde et al. (2013). The covariance matrices have been estimated in Boera et al. (2019) from the data, using “bootstrap method”. While bootstrap method is widely used in the literature for estimating the covariance matrix, it can only evaluate covariance due to the scatter within the sample (see *e.g.*, Rollinde et al. (2013)). From the data one cannot estimate, however, how representative the sample is – this contribution is also commonly called *sample variance*. Because of the smallness of the sample size the sample variance can be an important contribution to the covariance matrix. We try to estimate it using the simulations. To properly recover a covariance matrix from the simulations, one needs a simulation box whose size is comparable with the comoving length of the spectra (see *e.g.*, discussion in Garzilli et al. (2019)). A typical length of a single Lyman- α forest spectrum is ~ 200 cMpc, while our simulation box is 20 cMpc.

In order to evaluate the covariance matrix we took the EAGLE simulation with $L = 100$ Mpc/h and $N_{\text{part}} = 1504^3$ (Schaye et al. 2015). These simulations do not have the resolution needed for the

² The details about the numerical simulations can be found in (Garzilli et al. 2019).

³ We thank J. Oñorbe for sharing with us the data of the LATECOLD thermal history that were not published together with the other thermal histories in Oñorbe et al. (2017a).

Name	L [Mpc/ h]	N	Dark matter	UVB
CDM	20	1024^3	CDM	LATECOLD
WDM	same	same	$m_{\text{WDM}} = 2 \text{ keV}$	same
EAGLE_REF	$100 h$	1504^3	CDM	EAGLE

Table 1. Hydrodynamical simulations considered in this work together with corresponding parameters. All simulations were performed specifically for this work, except EAGLE_REF (Schaye et al. 2015). Columns contain from left to right: simulation identifier, co-moving linear extent of the simulated volume (L), number of dark matter particles (N ; also equal to the number of gas particles), type of dark matter (CDM or WDM), m_{WDM} (expressed in natural units), ultra-violet background imposed during the simulation (LATECOLD refers to a reionization model in agreement with measured temperature of the IGM as discussed in Oñorbe et al. (2017a), see Fig. 1; EAGLE indicates the standard UVB from (Haardt & Madau 2001)). The cosmological parameters are chosen according to Table 2. The gravitational softening length for gas and dark matter is kept constant in co-moving coordinates at $1/30^{\text{th}}$ of the initial interparticle spacing. All simulations start from the initial conditions generated by the 2LPTic (Scoccimarro et al. 2012) with the same ‘glass’-like particle distribution generated by GADGET-2 (Springel 2005).

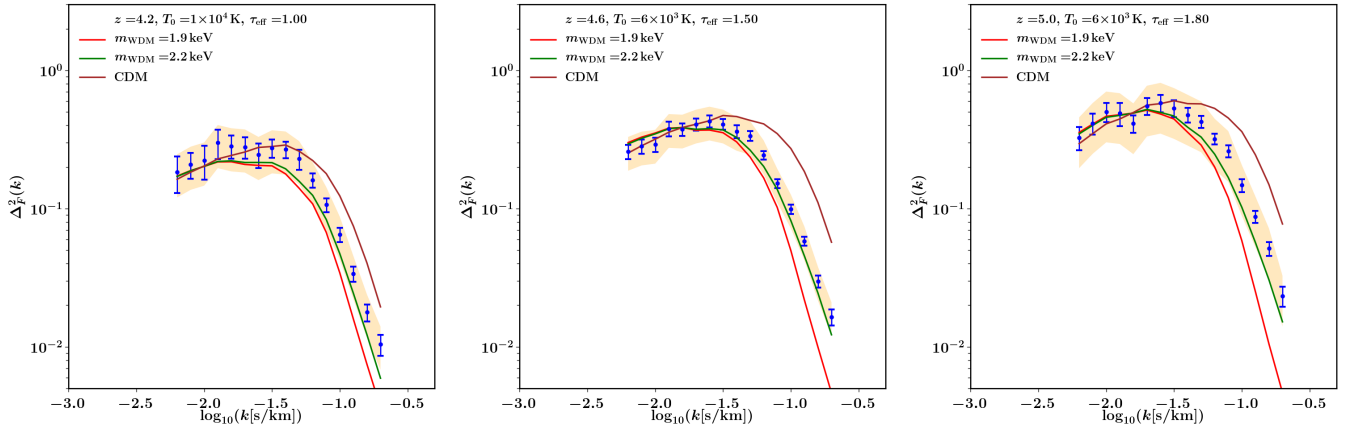


Figure 2. Data of Boera et al. together with several cosmological models: WDM with $m_{\text{WDM}} = 1.9 \text{ keV}$ (red line, compatible with the data at 95% CL), WDM with $m_{\text{WDM}} = 2.2 \text{ keV}$ (green line) and CDM (brown line). The thermal history LATECOLD from Oñorbe et al. (2017a) with late redshift of reionization $z_{\text{reio}} = 6.7$ is used for all three models. Orange shaded region indicates the level of uncertainty of the data, related to the sample variance (estimated from the simulations, see text for details).

Cosmology	<i>Planck</i> (Ade et al. 2016)
Ω_0	0.308 ± 0.012
Ω_Λ	0.692 ± 0.012
$\Omega_b h^2$	0.02226 ± 0.00023
h	0.6781 ± 0.0092
n_s	0.9677 ± 0.0060
σ_8	0.8149 ± 0.0093

Table 2. Cosmological parameters used in our simulations. *Planck* cosmology is the conservative choice of TT+lowP+lensing from Ade et al. (2016) (errors represent 68% confidence intervals).

smallest scales measured in the dataset (see the discussion in Garzilli et al. 2019). For this reason, we approximate the covariance matrix with the following procedure. We computed the expected covariance matrix from the above mentioned EAGLE simulation run by bootstrap, considering a mock data sample of the length equivalent to that of the observed data sample. For each redshift interval, we consider the snapshot at the central redshift. We extract 1000 mock spectra. We compute the FPS for each mock spectrum. We group the mock spectra in sub-samples with the same comoving length as the data-sample, and for each mock sub-sample we compute the average of the FPS. The covariance matrix is computed with the average FPS

with respect to the average FPS computed on all the mock spectra. After that, we compute the maximum relative errors obtained by comparing the diagonal elements of the covariance matrix to the data. Hence, we rescale all elements of the covariance matrix to this same maximum relative error. Our normalized matrices does not coincide with those of (Boera et al. 2019), but their diagonal terms are comparable in magnitude, the difference can be attributed to a different resolution. Indeed, we checked that insufficient resolution *increases* a correlation between data points.

In Figure 2 we show a direct comparison between the data and three distinct cosmologies with LateCold thermal history. While the WDM cosmology with $m_{\text{WDM}} = 2.2 \text{ keV}$ is excluded at $2\text{-}\sigma$, the WDM cosmology with $m_{\text{WDM}} = 1.9 \text{ keV}$ is compatible with the data at 95% CL, and the CDM cosmology is compatible with the data. The reason is that we claim that all the models whose flux PS lies below the observed flux PS must be excluded in our analysis. In fact, among all the thermal histories that are compatible with the observations, we have considered the thermal history that provide the minimal filtering length. Hence a model whose flux PS lies below the observations cannot become compatible with the data with another thermal history. Instead a model whose flux PS is above the observations may be compatible with the data if another thermal history is considered.

parameter	lower range	upper range
$1/m_{\text{WDM}} [1/\text{keV}]$	0	1
$T_0(z = 4.2) [\text{K}]$	10^3	10^4
$T_0(z = 4.6) [\text{K}]$	10^3	10^4
$T_0(z = 5.0) [\text{K}]$	10^3	10^4
$\tau_{\text{eff}}(z = 4.2)$	0.5	2.0
$\tau_{\text{eff}}(z = 4.6)$	0.5	2.0
$\tau_{\text{eff}}(z = 5.0)$	0.5	2.0

Table 3. We show the priors that have been considered in our analysis.

2.2 Data analysis

Our resulting model describing evolution of FPS contains 7 parameters: inverse WDM mass $[1/\text{keV}]/m_{\text{WDM}}$, IGM temperature at the cosmic mean density and τ_{eff} (the latter two quantities are evaluated at redshifts $z = 4.2, 4.6, 5.0$). We consider linear priors on the temperature and logarithmic priors on the mass of warm dark matter. In order to get theoretical predictions of the FPS, we run our simulations for two distinct cosmological models: CDM, and thermal relic WDM with mass 2 keV. Starting from our simulations, we compute in post-processing the FPS in k -space for each set of the parameters, the parameters are three and they are arranged on a three-dimensional regular grid. Our final theoretical model is obtained by interpolating linearly the FPS across the grid. We perform a joint analysis on all the redshift intervals.

3 RESULTS

We explore the likelihood via the Monte Carlo Markov Chains (MCMC). The priors are shown in Table 3. The 1σ and 2σ contours of the cosmic mean temperature, T_0 , the optical depth, τ , and the mass of the WDM, m_{WDM} are shown in Figure 3. By marginalizing over $T_0(z)$ and $\tau(z)$ we find the lower limit on the warm dark matter $m_{\text{WDM}} \geq 1.9 \text{ keV}$ at 95% CL. Warmer WDM models are excluded regardless of the instantaneous temperature of IGM, as the contours in Fig. 3 demonstrate. For each mass we also find the *upper bound* on $T_0(z)$ at redshifts $z = 4.2, 4.6, 5.0$, see Fig. 4. A complete set of 2D plots are shown in Fig. 6. We have repeated the MCMC exploration using the covariance matrix provided by Boera et al. (2019), albeit with the errorbars inflated to account for the sample variance. The resulting contours changed only slightly with the 95% CL for the mass reaching 2.05 keV.

As our procedure is somewhat different from a standard MCMC exploration of the likelihood, we have several comments:

- (i) Our contours do not reach the CDM values ($1/m_{\text{WDM}} = 0$). This does not mean that the CDM cosmology is excluded by the data. This indicates that in the LATECOLD reionization scenario with cold DM, the temperature alone would not be sufficient to explain the suppression of the FPS. For this reason, we only consider the upper portion of the contours that are depicted in Figure 3. Therefore, in CDM cosmology the LATECOLD model would be ruled out, while in the WDM cosmology with $m_{\text{WDM}} > 1.9 \text{ keV}$ it is actually allowed. Ref. Walther et al. (2019) studied the dataset of Viel et al. (2013) and found that cold DM model with LATECOLD reionization is consistent with the data, but they did not study the dataset Boera et al. (2019) we have considered in this work.
- (ii) For the same reason our upper limits on the temperature (Fig. 4) are, probably, exaggerated as they compensate minimal pressure history. While for the LATECOLD history these are 95% CL upper

bounds, for other thermal histories at similar confidence level one would be getting lower temperatures. Thus, one can treat them as (overly) conservative upper bounds on T_0 . We do not provide lower bounds on the temperature as they are not meaningful.

4 CONCLUSION AND FUTURE WORK

We have produced new constraint on the mass of warm dark matter particles using the high resolution Lyman- α forest dataset (Boera et al. 2019). In order to minimize astrophysical effects and to leave the room for warm dark matter, we have used a conservative IGM thermal history that gives a minimal size of the intergalactic structures (the smallest pressure effects). We have also explicitly marginalized over the Doppler broadening, finding that WDM thermal relics with mass as low as 1.9 keV are consistent with the data at 95% CL. Our procedure lowers the Lyman- α bound significantly compared to $m_{\text{WDM}} \geq 3.3 \text{ keV}$ obtained from the HIRES/MIKE data by Viel et al. (2013) (for detailed comparison between assumed thermal histories in these works see the discussion in Garzilli et al. (2017); Garzilli et al. (2019)).⁴ In terms of the characteristic free-streaming length, λ_{DM} our bound is two times weaker.

Our result does not include marginalization over other astrophysical “nuisance” parameters: a powerlaw index γ in the temperature-density relation (1), the AGN feedback, fluctuations of UVB, etc. In Fig. 5 we show that the difference between two highly distinct γ values can be compensated by the different choice of τ_{eff} , both consistent with measurements. Other effects have been explored in other works (see e.g. Bertone & White 2006; Becker et al. 2015; Garzilli et al. 2017; D’Aloisio et al. 2018; Chabanier et al. 2019; Wu et al. 2019; Sanderbeck & Bird 2020). We stress that our goal was not to provide a most robust bound on WDM mass, but rather to assess a level of systematic uncertainty as one varies the pressure support scale.

Because we have chosen a thermal history that minimize the cut-off on the flux PS, our bound is independent of the reionization history.

Although the difference between CDM and WDM is the most pronounced at small scales, the influence of astrophysical effects is also the largest there. Therefore, it becomes interesting to compare our results with those, obtained from the medium resolution SDSS Lyman- α forest datasets. These data have several advantages that may help to reduce this systematic uncertainty: reduced sample variance due to the large number of quasars; less pronounced dependence on astrophysical processes on larger scales. Using the SDSS dataset, Seljak et al. (2006) found $m_{\text{WDM}} \gtrsim 2.5 \text{ keV}$ (Viel et al. 2006, see also), which ref. Boyarsky et al. (2009a) reduced to $m_{\text{WDM}} \geq 1.7 \text{ keV}$, using a more conservative treatment of the systematic uncertainties. The most recent analysis based on the SDSS-III/BOSS dataset Baur et al. (2016, 2017) found $m_{\text{WDM}} \geq 3.06 \text{ keV}$ (when using Planck cosmological parameters). These works did not explore the influence of the thermal histories similar to LATECOLD used here, as discussed in the Introduction. We leave investigation of this question for a future work.

In this work we adopted LATECOLD reionization history as the one, providing minimal pressure support, consistent with existing data. Whether this is the case in non-CDM cosmologies (not explored in Oñorbe et al. (2017a)) or whether minimal pressure scale λ_p can be estimated by other methods (e.g., Garzilli et al. (2015, 2020)) or from other data (see e.g., Telikova et al. (2019)) remains to be seen.

⁴ All limits quoted at this section are at 95% CL.

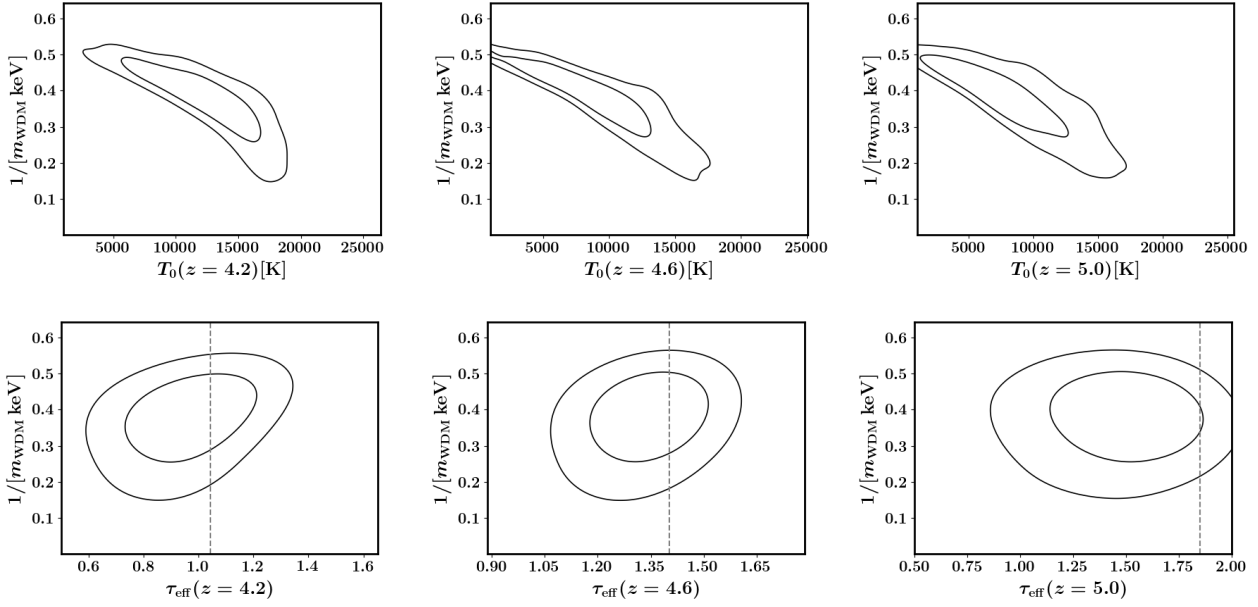


Figure 3. Confidence regions between the WDM mass, m_{WDM} , the IGM mean temperature, T_0 and the effective optical depth τ_{eff} at redshifts $z = 4.2, 4.6, 5.0$, the T_0 upper bound limits are still dependent on the specific choice of the pressure smoothing model. Our analysis shows that if LATECOLD were a true history of reionization, then the CDM would be ruled out. However, it is not possible to use this analysis to determine the IGM temperature in CDM for reionization histories outside LATECOLD. For the same reason our analysis does not allow to determine robust *lower* bounds on T_0 for a given WDM mass. The (conservative) upper bounds are shown in Fig. 4.

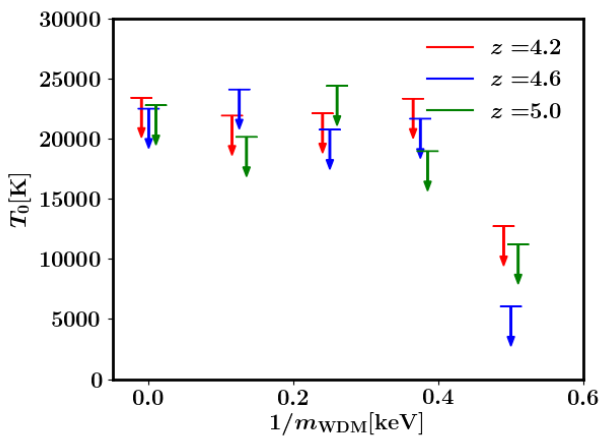


Figure 4. The $2\text{-}\sigma$ level upper limit on T_0 as a function of $1/m_{\text{WDM}}$. The upper limit has been estimated separately for each redshift interval with fixed m_{WDM} . We only show the mass interval between $m_{\text{WDM}} = 2$ keV and CDM. This result is in substantial agreement with the global fit that we have shown in Figure 3. These bounds are fully consistent with existing estimates of the IGM temperatures at redshifts $z = 4 - 5$ (see *e.g.*, Schaye et al. 2000; Becker et al. 2007; Becker et al. 2011; Bolton et al. 2012). One should keep in mind that these works evaluated IGM temperatures for CDM cosmology only and for some limited class of thermal histories, not necessarily consistent with LATECOLD.

We note that there are many other bounds on WDM, not based on the Lyman- α forest data (for example, those based on gravitational lensing (Hsueh et al. 2020), stellar streams (Banik et al. 2019), satellite counts (Nadler et al. 2020)), each of them claiming bounds

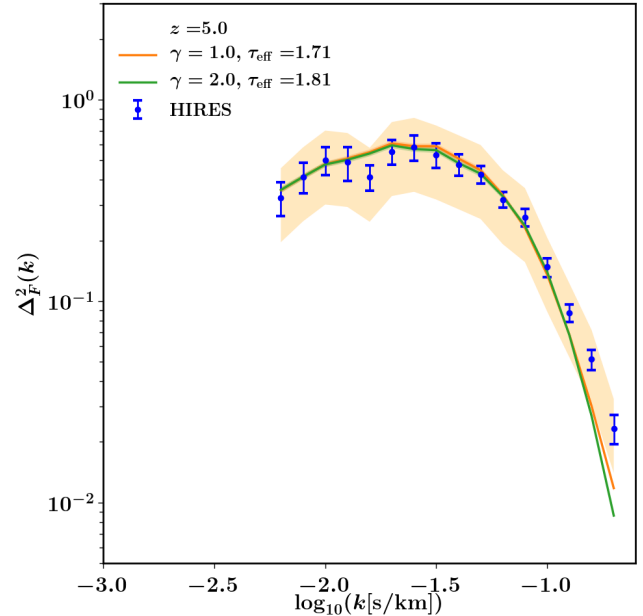


Figure 5. Dependence of the flux power spectrum on gamma can be ignored, given a poorly constrained overall normalization τ_{eff} .

of $\lambda_{\text{DM}} \lesssim O(10 - 30)$ kpc. At these small scales the influence of baryonic physics is significant (even dominant) and each of these bounds suffer from their own systematic uncertainties. Therefore, it is important to assess the systematic uncertainty of each of the methods. Our work makes the first step in this direction for the Lyman- α forest method.

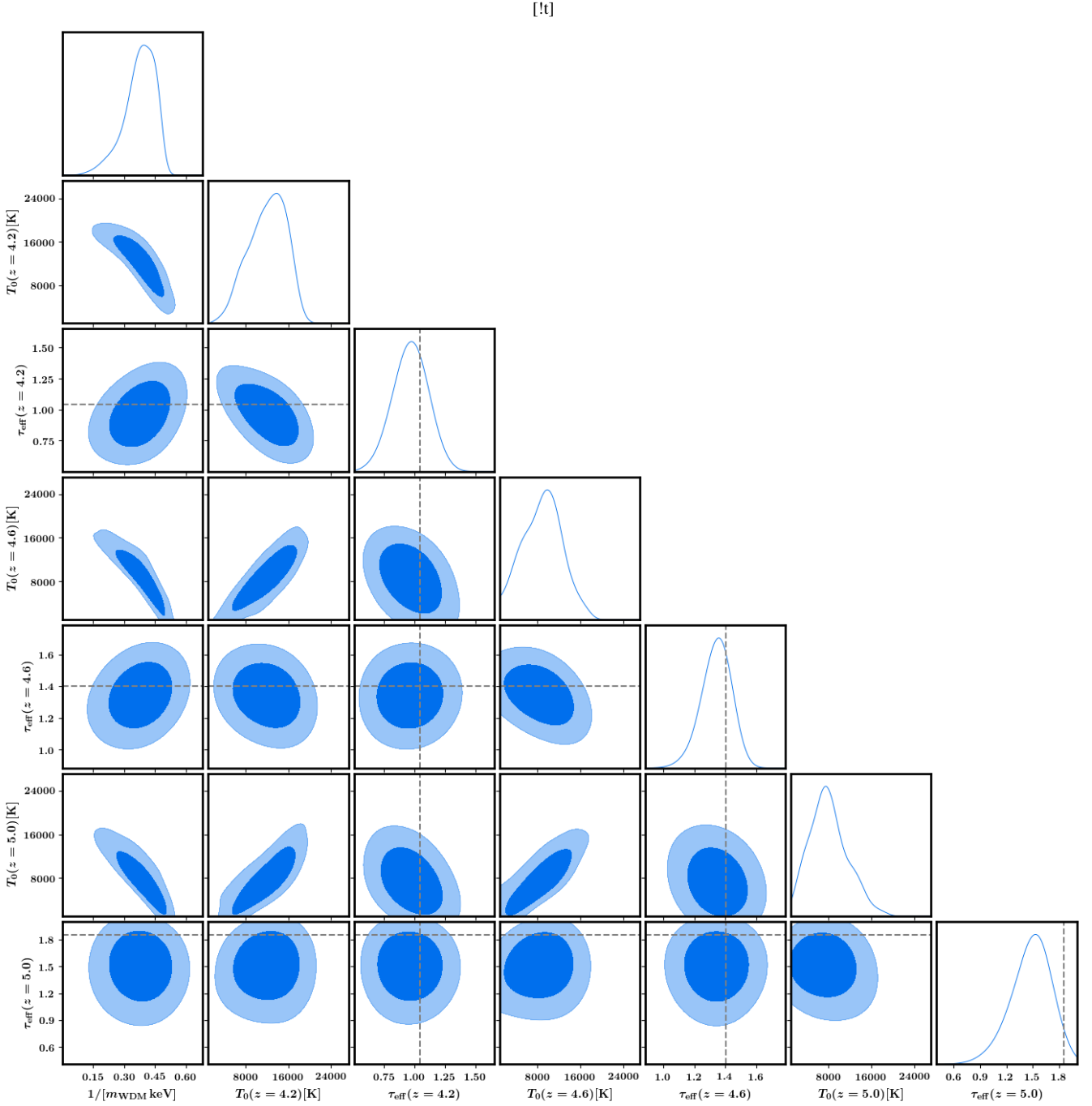


Figure 6. Confidence regions between the WDM mass, m_{WDM} , the IGM mean temperature, T_0 and the effective optical depth, τ_{eff} , at redshifts $z = 4.2, 4.6, 5.0$. The dashed grey lines are the τ_{eff} as measured in (Boera et al. 2019).

Acknowledgments. This project has received funding from the European Research Council (ERC) under the European Union’s Horizon 2020 research and innovation programme (ERC Advanced Grant 694896). This work used the DiRAC Data Centric system at Durham University, operated by the Institute for Computational Cosmology on behalf of the STFC DiRAC HPC Facility (www.dirac.ac.uk). This equipment was funded by BIS National E-infrastructure capital grant ST/K00042X/1, STFC capital grants ST/H008519/1 and ST/K00087X/1, STFC DiRAC Operations grant ST/K003267/1 and

Durham University. DiRAC is part of the National E-Infrastructure. AM is supported by the Netherlands Organization for Scientific Research (NWO) under the program "Observing the Big Bang" of the Organization for Fundamental Research in Matter (FOM).

We would like to thank Jose Oñorbe for sharing with us additional unpublished thermal histories.

Data availability. The data that support the findings of this study are available from the corresponding author, A.G., upon reasonable request.

REFERENCES

- Ade P. A. R., et al., 2016, *Astron. Astrophys.*, 594, A13
- Banik N., Bovy J., Bertone G., Erkal D., de Boer T. J. L., 2019
- Baur J., Palanque-Delabrouille N., Yèche C., Magneville C., Viel M., 2016, *J. Cosmology Astropart. Phys.*, 8, 012
- Baur J., Palanque-Delabrouille N., Yèche C., Boyarsky A., Ruchayskiy O., Armengaud É., Lesgourgues J., 2017, *J. Cosmology Astropart. Phys.*, 12, 013
- Becker R. H., et al., 2001, *Astron. J.*, 122, 2850
- Becker G. D., Rauch M., Sargent W. L. W., 2007, *Astrophys. J.*, 662, 72
- Becker G. D., Bolton J. S., Haehnelt M. G., Sargent W. L. W., 2011, *Mon. Not. Roy. Astron. Soc.*, 410, 1096
- Becker G. D., Bolton J. S., Madau P., Pettini M., Ryan-Weber E. V., Venemans B. P., 2015, *Mon. Not. Roy. Astron. Soc.*, 447, 3402
- Bernstein G. M., Athey A. E., Bernstein R., Gunnels S. M., Richstone D. O., Shectman S. A., 2002, Volume-phase holographic spectrograph for the Magellan telescopes. pp 453–459, doi:10.1117/12.454281
- Bertone S., White S. D. M., 2006, *Mon. Not. Roy. Astron. Soc.*, 367, 247
- Bode P., Ostriker J. P., Turok N., 2001, *Astrophys. J.*, 556, 93
- Boera E., Becker G. D., Bolton J. S., Nasir F., 2019, *Astrophys. J.*, 872, 101
- Bolton J. S., Becker G. D., Wyithe J. S. B., Haehnelt M. G., Sargent W. L. W., 2010, *Mon. Not. Roy. Astron. Soc.*, 406, 612
- Bolton J. S., Becker G. D., Raskutti S., Wyithe J. S. B., Haehnelt M. G., Sargent W. L. W., 2012, *Mon. Not. Roy. Astron. Soc.*, 419, 2880
- Boyarsky A., Lesgourgues J., Ruchayskiy O., Viel M., 2009a, *J. Cosmology Astropart. Phys.*, 5, 012
- Boyarsky A., Lesgourgues J., Ruchayskiy O., Viel M., 2009b, *Phys. Rev. Lett.*, 102, 201304
- Chabanier S., et al., 2019, *J. Cosmology Astropart. Phys.*, 1907, 017
- D’Aloisio A., McQuinn M., Davies F. B., Furlanetto S. R., 2018, *Mon. Not. Roy. Astron. Soc.*, 473, 560
- Gaikwad P., et al., 2020, *Mon. Not. Roy. Astron. Soc.*, 494, 5091
- Garzilli A., Theuns T., Schaye J., 2015, *Mon. Not. Roy. Astron. Soc.*, 450, 1465
- Garzilli A., Boyarsky A., Ruchayskiy O., 2017, *Phys. Lett.*, B773, 258
- Garzilli A., Magalich A., Theuns T., Frenk C. S., Weniger C., Ruchayskiy O., Boyarsky A., 2019, *Mon. Not. Roy. Astron. Soc.*, p. 2103
- Garzilli A., Theuns T., Schaye J., 2020, *Mon. Not. Roy. Astron. Soc.*, 492, 2193
- Gnedin N. Y., Hui L., 1998, *Mon. Not. Roy. Astron. Soc.*, 296, 44
- Haardt F., Madau P., 2001, in Neumann D. M., Tran J. T. V., eds, Clusters of Galaxies and the High Redshift Universe Observed in X-rays. ArXiv astro-ph/0106018 (arXiv:astro-ph/0106018)
- Haardt F., Madau P., 2012, *Astrophys. J.*, 746, 125
- Hansen S. H., Lesgourgues J., Pastor S., Silk J., 2002, *Mon. Not. Roy. Astron. Soc.*, 333, 544
- Hsueh J.-W., Enzi W., Vegetti S., Auger M., Fassnacht C. D., Despali G., Koopmans L. V. E., McKean J. P., 2020, *Mon. Not. Roy. Astron. Soc.*, 492, 3047
- Hui L., Haiman Z., 2003, *Astrophys. J.*, 596, 9
- Hui L., Rutledge R. E., 1999, *Astrophys. J.*, 517, 541
- Iršič V., et al., 2017, *Phys. Rev. D*, 96, 023522
- Kulkarni G., Hennawi J. F., Oñorbe J., Rorai A., Springel V., 2015, *Astrophys. J.*, 812, 30
- Lidz A., Malloy M., 2014, *Astrophys. J.*, 788, 175
- Meiksin A. A., 2009, *Rev. Mod. Phys.*, 81, 1405
- Murgia R., Iršič V., Viel M., 2018, ArXiv preprint 1806.08371
- Nadler E. O., et al., 2020
- Oñorbe J., Hennawi J. F., Lukić Z., 2017a, *Astrophys. J.*, 837, 106
- Oñorbe J., Hennawi J. F., Lukić Z., Walther M., 2017b, *Astrophys. J.*, 847, 63
- Palanque-Delabrouille N., Yèche C., Schöneberg N., Lesgourgues J., Walther M., Chabanier S., Armengaud E., 2020, *JCAP*, 2004, 038
- Peebles P. J. E., 2017, *Nat. Astron.*, 1, 0057
- Rollinde E., Theuns T., Schaye J., Pâris I., Petitjean P., 2013, *Mon. Not. Roy. Astron. Soc.*, 428, 540
- Rorai A., Carswell R. F., Haehnelt M. G., Becker G. D., Bolton J. S., Murphy M. T., 2018, *Mon. Not. Roy. Astron. Soc.*, 474, 2871
- Sanderbeck P. U., Bird S., 2020, J 10.1093/mnras/staa1850
- Schaye J., Theuns T., Rauch M., Efstathiou G., Sargent W. L. W., 2000, *Mon. Not. Roy. Astron. Soc.*, 318, 817
- Schaye J., Crain R. A., Bower R. G., al. 2015, *Mon. Not. Roy. Astron. Soc.*, 446, 521
- Schroeder J., Mesinger A., Haiman Z., 2013, *Mon. Not. Roy. Astron. Soc.*, 428, 3058
- Scoccimarro R., Hui L., Manera M., Chan K. C., 2012, *Phys. Rev. D*, 85, 083002
- Seljak U., Makarov A., McDonald P., Trac H., 2006, *Phys. Rev. Lett.*, 97, 191303
- Springel V., 2005, *Mon. Not. Roy. Astron. Soc.*, 364, 1105
- Telikova K. N., Balashev S. A., Shternin P. S., 2019, *J. Phys. Conf. Ser.*, 1400, 022024
- Theuns T., Schaye J., Haehnelt M. G., 2000, *Mon. Not. Roy. Astron. Soc.*, 315, 600
- Upton Sanderbeck P. R., D’Aloisio A., McQuinn M. J., 2016, *Mon. Not. Roy. Astron. Soc.*, 460, 1885
- Viel M., Lesgourgues J., Haehnelt M. G., Matarrese S., Riotto A., 2005, *Phys. Rev.*, D71, 063534
- Viel M., Lesgourgues J., Haehnelt M. G., Matarrese S., Riotto A., 2006, *Phys. Rev. Lett.*, 97, 071301
- Viel M., Becker G. D., Bolton J. S., Haehnelt M. G., Rauch M., Sargent W. L. W., 2008, *Phys. Rev. Lett.*, 100, 041304
- Viel M., Becker G. D., Bolton J. S., Haehnelt M. G., 2013, *Phys. Rev. D*, 88, 043502
- Vogt S. S., et al., 1994, *Proc. SPIE Int. Soc. Opt. Eng.*, 2198, 362
- Walther M., Hennawi J. F., Hiss H., Oñorbe J., Lee K.-G., Rorai A., O’Meara J., 2018, *Astrophys. J.*, 852, 22
- Walther M., Oñorbe J., Hennawi J. F., Lukić Z., 2019, *Astrophys. J.*, 872, 13
- Wu X., McQuinn M., Kannan R., D’Aloisio A., Bird S., Marinacci F., Davé R., Hernquist L., 2019, *Mon. Not. Roy. Astron. Soc.*, 490, 3177